Eur J Nucl Med Mol Imaging
DOI 10.1007/s00259-010-1422-4

GUIDELINES

EANM Dosimetry Committee guidelines for bone marrow and whole-body dosimetry

Cecilia Hindorf · Gerhard Glatting · Carlo Chiesa · Ola Lindén · Glenn Flux

Abstract
Introduction The level of administered activity in radionuclide therapy is often limited by haematological toxicity resulting from the absorbed dose delivered to the bone marrow. The purpose of these EANM guidelines is to provide advice to scientists and clinicians on data acquisition and data analysis related to bone-marrow and whole-body dosimetry.

Materials and methods The guidelines are divided into sections "Data acquisition" and "Data analysis". The Data acquisition section provides advice on the measurements required for accurate dosimetry including blood samples, quantitative imaging and/or whole-body measurements with a single probe. Issues specific to given radiopharmaceuticals are considered. The Data analysis section provides advice on the calculation of absorbed doses to the whole body and the bone marrow. The total absorbed dose to the bone marrow consists of contributions from activity in the bone marrow itself (self-absorbed dose) and the cross-absorbed dose to the bone marrow from activity in bone, larger organs and the remainder of the body.
Conclusion As radionuclide therapy enters an era where patient-specific dosimetry is used to guide treatments, accurate bone-marrow and whole-body dosimetry will become an essential element of treatment planning. We hope that these guidelines will provide a basis for the optimization and standardization of the treatment of cancer with radiopharmaceuticals, which will facilitate single- and multi-centre radionuclide therapy studies.

Keywords Internal dosimetry · Radionuclide therapy · Bone marrow

These guidelines summarize the views of the Dosimetry Committee of the EANM and reflects recommendation for which the EANM cannot be held responsible. The guidelines have been reviewed by the EANM Radionuclide Therapy Committee and the EANM Physics Committee and they have been brought to the attention of the National Societies of Nuclear Medicine. The recommendations should be taken in the context of good practice of nuclear medicine and do not substitute for national and international legal or regulatory provisions.

C. Hindorf (✉)
Imagerie Médicale, ONIRIS - Ecole Nationale Vétérinaire, Agroalimentaire et d'Alimentation Nantes Atlantique, Atlanpole, La Chantrerie, BP 40706, 44307 CEDEX 3 Nantes, France
e-mail: cecilia.hindorf@oniris-nantes.fr

G. Glatting
Klinik für Nuklearmedizin, Universität Ulm, Ulm, Germany

C. Chiesa
Nuclear Medicine Division, Foundation IRCCS Istituto Nazionale Tumori, Milano, Italy

O. Lindén
Department of Oncology, Lund University Hospital, Lund, Sweden

G. Flux
Joint Department of Physics, Royal Marsden Hospital & Institute of Cancer Research, London, UK

Introduction

The ultimate goal of bone marrow dosimetry is to predict the level of toxicity from radionuclide therapy and thereby deliver the most efficient therapy with a minimal level of adverse effects for the patient. Bone marrow is the most radiosensitive tissue in the body and without stem cell support it is commonly the dose-limiting tissue for radionuclide therapy. Toxicity can be predicted via the

Published online: 22 April 2010

establishment of the relationships between absorbed dose and biological effect which must be established separately for each radiopharmaceutical and for each patient subgroup. The calculation of absorbed dose to red bone marrow is also important in the application of radionuclide therapy to conditioning prior to stem cell transplantation. Stem cell support given either too early or too late will delay the patient's recovery or even jeopardize it. Early support will incur unnecessary irradiation and damage to the injected cells from activity circulating in the blood and the bone marrow or prevent successful engraftment, whilst late stem cell support would delay the patient's haematological recovery and translate into increased medical risks and higher treatment costs.

Demonstration of the relationships between absorbed dose and biological effect for bone marrow toxicity from radionuclide therapy have proven elusive, although it is likely that these exist for radionuclide therapy also. The existence of such a relationship can be inferred from the need for bone marrow support at higher administered activities and the dependence of bone marrow toxicity on the whole-body absorbed dose for ^{131}I-tositumomab (Bexxar©) [1]. The individual sensitivity and biological effects caused by previous treatments can confound the search for correlations, especially as the dosimetry studies performed to date [2–10] have commonly included few patients. Studies involving larger cohorts in multicentre settings are essential to determine the relationship as the relative standard deviation of the absorbed dose and the biological effect would decrease. The establishment of guidelines will facilitate multicentre studies and enable direct comparisons of results.

Bone marrow

The bone marrow is part of the skeleton and is spread throughout the body, situated within the cavities of the bones. The total weight of the bone marrow is approximately 5.0% of the whole body weight or 3,650 g for a healthy adult male man [11]. Approximately one-third of the total bone marrow is red marrow (1,170 g in men, 900 g in women), which is the haematopoietically active tissue, and the rest is yellow marrow (2,480 g in men, 1,800 g in women), which mainly consists of fat and does not actively produce any blood cells. Figures for bone marrow weight mentioned above apply to the ICRP reference man [12]. All of the bone marrow is active in the newborn. The relative percentage between red and yellow marrow changes with age, and the spatial distribution of red marrow within the body also changes, from being present in almost all skeletal bones at birth to being mainly present in the ribs (16.1%), the thoracic vertebrae (16.1%), the lumbar vertebrae (12.3%), the sacrum (9.9%) and the os coxae (17.5%) in the adult [11, 13]. The percentages in parentheses represent the percentage of total red marrow present at the respective sites in a 40-year-old human.

All blood cells are produced in the red marrow and originate from one single type of stem cell. In order to maintain homeostasis 490×10^9 blood cells are, on average, produced and removed from the body per day [14]. Although the bone marrow is distributed throughout the body it is regulated as one organ/tissue which can explain the redistribution of blood cell production after regional irradiation. Each stem cell is in the resting G_0 state more than 90% of the time and can start to replicate if needed. It has been suggested that an intact microenvironment is as important as the survival of the stem cells for avoidance of haematological toxicity. The life-span of erythrocytes is approximately 120 days and the life-span for granulocytes, lymphocytes and platelets is 7–30 hours, 4.4 years and 9–12 days, respectively [15].

Dosimetry

The mean absorbed dose to a target region (k) is calculated by multiplying the number of disintegrations (the cumulated activity, $\widetilde{A}_h$) in a source region (h) and the absorbed dose to the target region per disintegration in the source region (the S value, $S_{k\leftarrow h}$). The total mean absorbed dose to a target region equals the sum of the contributions from all source regions:

$$\overline{D}_k = \sum_h \widetilde{A}_h \cdot S_{k\leftarrow h} \quad (1)$$

The formalism as described in the MIRD Primer [16] is utilized in this set of guidelines. A list of the symbols used is given in Table 1.

There are three groups of contributors (source regions of activity) to the mean absorbed dose to the bone marrow, $\overline{D}_{BM}$: activity in the bone marrow itself, activity in bone, and activity in major tissues and the remainder of the body. Furthermore, the macroscopic self-absorbed dose to the bone marrow can on a microscopic scale be further divided into the contributions from activity in bone marrow cells, activity on blood cells and activity in the extracellular fluid in the bone marrow.

1. Activity in bone marrow $\left(\overline{D}_{BM\leftarrow BM}\right)$
   a Activity in extracellular fluid $\left(\overline{D}_{BM\leftarrow ECF}\right)$
   b activity in blood or blood components $\left(\overline{D}_{BM\leftarrow BLcells}\right)$
   c activity in bone marrow cells $\left(\overline{D}_{BM\leftarrow BMcells}\right)$
2. Activity in bone $\left(\overline{D}_{BM\leftarrow bone}\right)$
3. Activity in major organs and the remainder of the body ($\sum_h \overline{D}_{BM\leftarrow h}$ and $\overline{D}_{BM\leftarrow RoB}$)

The respective fractional contributions depend on the pharmacokinetics of the radiopharmaceutical, on the dis-

Table 1 Symbols used in the equations and their definitions

Symbol	Definition
A_0	Administered activity
$A_h(t)$	Activity in the source region h as a function of time after administration
$[A]_h$	Activity concentration in the source region h
$\widetilde{A}_h$	Cumulated activity in source region h
$\left[\widetilde{A}_h\right]$	Cumulated activity concentration in the source region h
b	Source thickness
blood	Blood
BLcells	Blood cells present in the bone marrow
BM	Bone marrow
BMcells	Bone marrow cells
C	Measured background- and dead time-corrected count rate (counts per unit time)
d	Patient thickness
$\overline{D}_{k\leftarrow h}$	Mean absorbed dose to target region k from activity in source region h
$\overline{D}_k$	Total mean absorbed dose to target region k
f	Fraction of extrapolated contribution to the total cumulated activity
HCT	Haematocrit. The fraction of the total blood volume that is occupied by blood cells
K	Calibration factor, translating the count rate to activity
λ	Physical decay constant for the radionuclide ($\lambda=\ln(2)/T_{1/2}$)
$\lambda_{h,j}$	Biological disappearance constant for the jth exponential component of activity in source region h ($\lambda_{h,j}=\ln(2)/T_{1/2,h,j}$)
$m_{k,phantom}$	Mass of target region k for the phantom
$m_{k,patient}$	Mass of the target region k for the patient
plasma	Plasma
$r_{ROI,BM}$	Fraction of total bone marrow present in the region of interest (see Table 3)
$r_{ROI,bone}$	Fraction of total bone present in the region of interest (see Table 4)
RoB	Remainder of the body
RM	Red marrow
RMBLR	Ratio of the activity concentration in red marrow to blood
RMECFF	Red marrow extracellular fluid fraction
$S_{k\leftarrow h}$	S value. The absorbed dose to the target region k per decay in the source region h
t_1	First time point after the administration for data acquisition
t_T	Last time point after the administration for data acquisition
$T_{1/2}$	Physical half-life for the radionuclide
$T_{1/2,h,j}$	Biological half-time for the j-th exponential component
WB	Whole body

ease and on patient characteristics, for example the degree of bone marrow involvement in a lymphoma patient.

These guidelines provide the data acquisitions and calculations needed to perform bone marrow dosimetry. The guidelines consist of two main sections 'Data acquisition' and 'Data analysis'. The main section 'Data acquisition' is divided according to the type of data acquisition needed for a specific radiopharmaceutical, i.e. whole-body measurements, blood samples and quantitative imaging. The 'Data analysis' section describes how to calculate the self- and cross-absorbed doses from the measurements of activity, and is divided into three subsections corresponding to the source regions briefly described above: bone marrow (extracellular fluid, blood and bone marrow cells), bone, and the remainder of the body. The calculation of the whole-body absorbed dose, which has often been applied in the search for the relationships between absorbed dose and biological effect, is also described in this section.

Data acquisition

The activity in the whole body as a function of time (described in the section 'Whole body') should be assessed for all radiopharmaceuticals to enable whole-body dosimetry and to determine the activity in the remainder of the

body which is used in the calculation of the cross-absorbed dose to the bone marrow. The following two sections describe the measurements to perform if there is no specific uptake in bone, bone marrow or components of blood. The activity concentration in plasma alone can only be applied to bone marrow dosimetry (the self-absorbed dose) if there is no specific activity uptake in the components of the blood (section 'Blood sampling'). However, if this is the case, then the activity concentration in the blood must be utilized (section 'Blood sampling'). Nevertheless, quantitative imaging needs to be performed if there is specific uptake in either the bone or the bone marrow cells themselves (section 'Quantitative imaging'). An exception to the general rule on quantitative imaging is for radiopharmaceuticals that are only distributed in one single organ/tissue (so that the activity in the whole body is equal to the activity in this single organ, for example bone). The data to be acquired and the source regions to be included for some common radiopharmaceuticals in clinical practice are listed in Table 2. It must be stressed that the list is general and that each case must be judged separately as the pharmacokinetics depend on several factors including the choice of radiopharmaceutical, the in vivo stability of the radiolabelling, the amount of metastatic spread to bone or to bone marrow, and also the specific features of each patient. Figure 1 gives a flow chart detailing the data required for bone-marrow dosimetry for radiopharmaceuticals not included in Table 2.

Number and timing of measurements The total number of time points needed for data acquisition to fully describe the activity in a source region as a function of time after administration depends on the pharmacokinetics of the particular radiopharmaceutical administered to each individual patient. Similar considerations also apply to the spread in time of the data acquisitions needed to accurately describe the activity as a function of time. A general rule of thumb is to include at least three measurements for each biological uptake and/or elimination phase for the source region in question [17].

Care must be taken to ensure that the activity as a function of time after administration is accurately determined from the measurements. Also, poorly chosen timing of measurements could hide an elimination phase and thereby give the wrong cumulated activity and absorbed dose. It is also necessary to choose the measurement time points to ensure that the contribution to the cumulated activity obtained from extrapolation from the first measurement back to the time of administration and from the last measurement to infinity is minimal. A method for the analysis of the above is presented in the section 'Data analysis' (Eq. 12).

Whole-body

The activity in the whole body as a function of time after administration can be assessed either from serial whole-body scans or from serial acquisitions by an external probe which allows a greater number of data points [18]. The first acquisition should be performed before any excretion of activity in order to normalize the number of counts to the

Table 2 Contributors to the total absorbed dose to bone marrow, $\overline{D}_{BM}$, for some radiopharmaceuticals used in radionuclide therapy. Note that quantitative imaging automatically gives the total activity present in the bone marrow, that is, the sum of the activity in the bone marrow cells, the activity in the blood cells present in the bone marrow and the activity freely circulating in the bone marrow

Group	Radiopharmaceutical	$\overline{D}_{BM}$				
		$\overline{D}_{BM\leftarrow BM}$			$\overline{D}_{BM\leftarrow bone}$	$\overline{D}_{BM\leftarrow RoB}$
		$\overline{D}_{BM\leftarrow BMcells}$	$\overline{D}_{BM\leftarrow ECF}$	$\overline{D}_{BM\leftarrow BLcells}$		
Monoclonal antibodies	^{90}Y/^{111}In-Zevalin	X[a]	X[c]	X	X[b]	X
	^{131}I-Bexxar	X[a]	X[c]	X		X
Peptides	^{90}Y-DOTATOC		X[c]	X	X[b]	X
	^{131}I-mIBG	X[a]	X[c]			X
Bone	^{89}Sr-Cl		X		X[d]	X
	^{153}Sm-EDTMP		X		X[d]	X
	^{186}Re-HEDP		X		X[d]	X
Thyroid	^{131}I-NaI		X			X

[a] Contribution of $\overline{D}_{BM\leftarrow BMcells}$ should be included if the patient has metastatic spread to the bone marrow.

[b] Free ^{90}Y is taken up in bone.

[c] Contribution of $\overline{D}_{BM\leftarrow ECF}$ should be included if the patient does not have metastatic spread to the bone marrow.

[d] The standard method results in large inaccuracies if the patient has considerable metastatic spread to the bone and has osteoporotic regions.

injected activity. Both anterior and posterior acquisitions should be performed at each acquisition time point. The total acquisition time for each measurement should ideally be chosen such that the background- and dead time-corrected number of counts is higher than 1×10^4 so that the statistical error is less than 1%.

The activity in the whole body at time T (t=T) after administration of the radiopharmaceutical ($A_{\mathrm{WB},t=T}$) is calculated as the product of the administered activity (A_0) and the normalized geometric mean of the anterior (C_{anterior}) and posterior ($C_{\mathrm{posterior}}$) count rates corrected for physical decay, background and dead time, as appropriate:

$$A_{WB,t=T} = A_0 \cdot \frac{\sqrt{C_{anterior,t=T} \cdot C_{posterior,t=T}}}{\sqrt{C_{anterior,t=0} \cdot C_{posterior,t=0}}} \quad (2)$$

Blood sampling

Activity in the bone marrow can be determined from the activity concentration in the blood or plasma if there is no specific uptake in the bone marrow cells. It is necessary to measure the activity concentration in the blood when there is uptake in any component of the blood, but if the activity is circulating freely in the plasma, the activity concentration in the plasma can be applied. However, ideally the activity concentration in the blood and plasma, as well as the patient's haematocrit (HCT, the proportion of the total blood volume that is occupied by blood cells), should be determined to allow certification of the absence of specific activity uptake in any component of the blood.

Blood samples should be drawn from the arm opposite the injection site to eliminate the risk of contamination. The

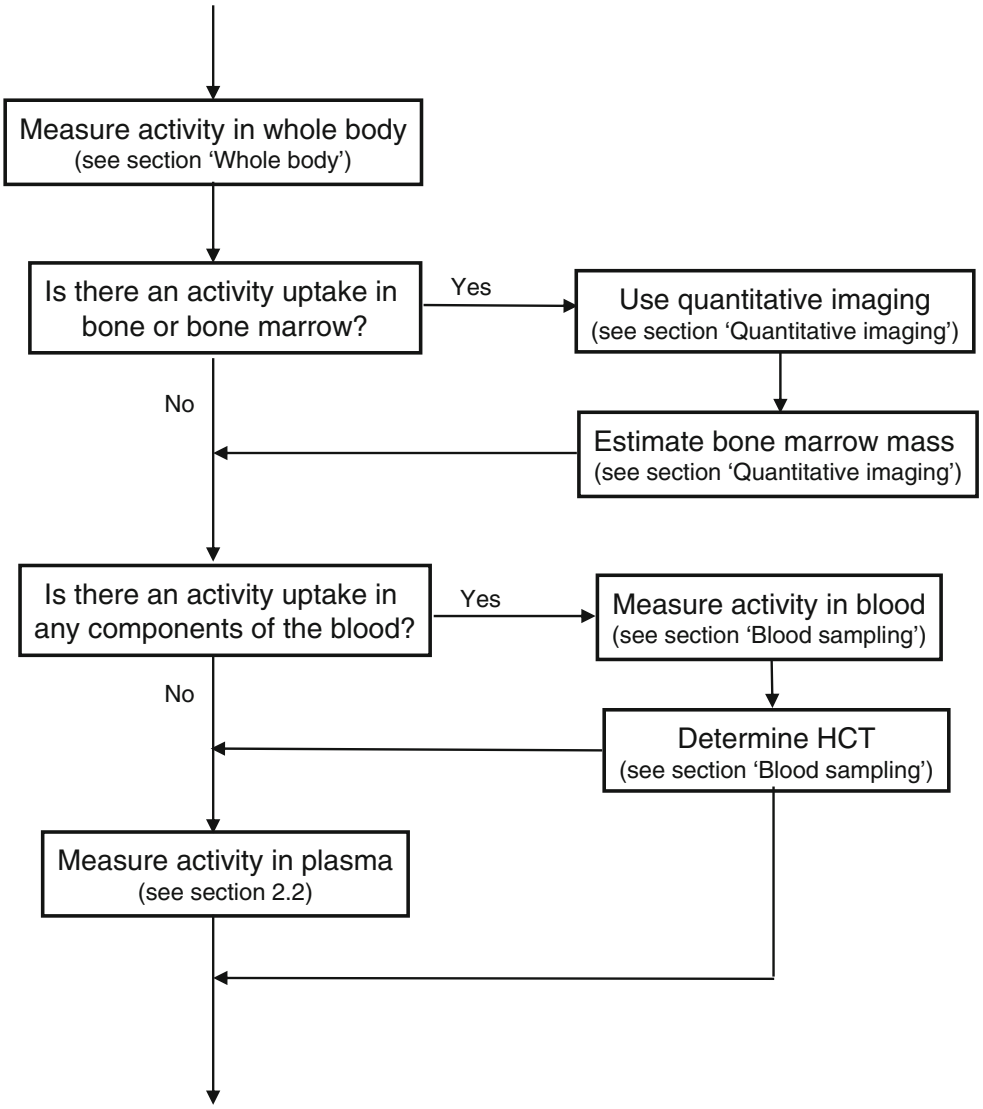

Fig. 1 Method for determining the data required to perform bone-marrow dosimetry

exact time point for the collection of each blood sample must be recorded. The timing and the total number of blood samples depends on the pharmacokinetics of the radiopharmaceutical in the body. The blood cells can be separated from the plasma by centrifugation.

Most commonly a well-type NaI(Tl) detector is used for the measurement of activity in the blood and/or plasma sample, but a beta counter or semiconductor detector could also be used. The response of the detector should be well characterized for the given radionuclide and measurement geometry so that corrections for sensitivity (count rate per unit activity), dead time and volume dependence (the self absorption of radiation in the sample and the geometry effects caused by differences in exposure of the sample to the detector) can be applied. Quenching should also be determined if a beta counter is used to determine the activity in blood as blood changes the absorption of the light produced in the scintillation liquid. Alternatively, a standard with a known amount of activity and of exactly the same volume as the blood/plasma samples can be measured together with the samples. The results for the standard can then be applied to convert the count rate of the blood/plasma samples into activity.

The volume of the blood (and/or plasma) sample should be determined either by weighing the empty and the full tube or by pipetting an exact preset volume into the tube. The acquisition time for measuring the activity should ideally be chosen so that the acquired, background-corrected, number of counts is higher than 10^4 so that the statistical inaccuracy is less than 1%.

Quantitative imaging

Quantitative imaging is the method of choice if the radiopharmaceutical has a specific uptake in either bone marrow or bone, although an exception to the rule is when all the activity in the whole body is taken up in one single tissue. The preferred methodology for quantitative imaging depends on many factors including the radioisotope, radiopharmaceutical, scintillation camera model and administered activity. Either planar (static images and/or whole-body scans) or SPECT acquisitions can be used for quantification of the activity. The inherent limitations of these two methods must be considered when setting up the study: a planar image cannot separate the activities in bone and bone marrow, and SPECT is limited by its relatively small field of view and, in general, has lower spatial resolution. A combination of planar scintillation camera imaging and SPECT may be preferable, and has previously been shown to be useful [19, 20]. The planar technique is applied to determining the shape of the curve describing the activity as a function of time after administration of the radiopharmaceutical and the SPECT image is utilized to determine the absolute activity at one time point and to normalize the activity as a function of time. Quantitative PET could also be applied [21–23], although it is not covered here as it is not yet established for dosimetry. An extensive review of quantitative imaging and multimodality imaging (SPECT/CT and PET/CT) is beyond the scope of these guidelines, but the following recommendations should be applicable to the vast majority of cases.

The choice of collimator and energy window settings should be matched according to the energy of the emitted photons. The matrix size and acquisition times should be balanced so as not to limit the spatial resolution, nor to keep the number of counts per pixel unnecessarily low. The effect of dead time for the scintillation camera must be corrected for. It is recommended that scatter is corrected for by, for example, the double or the triple energy window method [24, 25]. The contribution from scatter could also be accounted for by applying an effective attenuation coefficient, determined in broad-beam geometry for the radionuclide and scintillation camera settings applied, although if applicable the energy window methods are recommended.

The conjugate view method is the most common method for activity quantification and attenuation correction in planar images [17, 26, 27]. The conjugate view method requires anterior and posterior images as well as knowledge of the transmission factor $\left(e^{-\mu d/2}\right)$, which can be determined on a pixel level from a transmission scan or by recalculation of a CT scan, or for each region of interest (ROI) simply by knowledge of patient thickness at the site of the ROI (d) and the attenuation coefficient (μ). The narrow-beam attenuation coefficients for different energies and materials are tabulated, but the broad-beam attenuation coefficients (including scatter) should be determined experimentally for the given radionuclide, geometry and tissue. A calibration factor (k) to convert the count rate into activity must be determined for each scintillation camera, radionuclide and energy window setting. Activity in the source region at a given time point can be calculated from the counts according to the equation [28]:

$$A_{t=T} = k \cdot e^{\mu d/2} \cdot \sqrt{C_{anterior,t=T} \cdot C_{posterior,t=T}} \tag{3}$$

The conjugate view method assumes the source to be thin, without attenuation in the source itself, although it can be extended to take into account self-attenuation by adding an extra term [17]:

$$A_{t=T} = k \cdot e^{\mu d/2} \cdot \sqrt{C_{anterior,t=T} \cdot C_{posterior,t=T}} \cdot \frac{\mu b/2}{\sinh(\mu b/2)} \tag{4}$$

where b denotes the source thickness.

It should be noted that a high activity placed close to the surface could be more accurately determined by only one image and not by the geometric mean:

$$A_{t=T} = k \cdot e^{\mu x} \cdot C_{t=T,depth=x} \quad (5)$$

However, in this case the exact depth of the source (x) must be determined.

It is essential to correct for background counts as well as counts in over- and underlying tissues when planar images are quantified.

A uniform attenuation correction based on either analytical [29] or iterative [30, 31] reconstruction techniques should be applied to SPECT images.

ROIs for planar images or volumes of interest (VOIs) in SPECT images to determine the numbers of counts in certain regions of the image are typically drawn over the lumbar spine or sacrum, as large proportions of the red marrow are situated in these regions. However, ROIs/VOIs could be applied to all anatomical locations for bone marrow, as is important in the case of a pronounced nonuniform activity uptake. ROIs should be drawn large enough to include all counts pertinent to the anatomical region in question and to account for the partial volume effect. It is recommended that this is analysed in phantom images beforehand. The decrease in spatial resolution with increasing distance between the source and the collimator should also be accounted for.

Estimation of bone marrow mass

The S value ($S_{BM\leftarrow BM}$) should be scaled by mass to the patient-specific bone marrow mass, although this is difficult to determine accurately. Therefore, the patient-specific bone marrow mass ($m_{BM,patient}$) is usually estimated by a linear scaling of the reference man bone marrow mass ($m_{BM,phantom}$) by the whole body mass of the phantom ($m_{WB,phantom}$) and the patient ($m_{WB,patient}$):

$$m_{BM,patient} = m_{BM,phantom} \cdot \frac{m_{WB,patient}}{m_{WB,phantom}} \quad (6)$$

However, in obese patients it is more appropriate to replace the patient's whole body mass in Eq. 6 with the lean body mass [32].

Another method to estimate the patient-specific bone-marrow mass is via the spongiosa volume, that is the volume of the trabecular bone within which the active bone marrow is present [33]. A study by Shen et al. estimated the bone marrow mass from the volume of trabecular bone in the lumbar vertebrae (L2–L4) ($V_{trab,L2-L4,patient}$) on a CT scan [2]. The reference man trabecular bone volume ($V_{trab,L2-L4,phantom}$) was assumed to equal 70.3 ml which was the mean value of ($V_{trab,L2-L4,patient}$) for the patients included in the study:

$$m_{BM,patient} = m_{BM,phantom} \cdot \frac{V_{trab,L2-L4,patient}}{V_{trab,L2-L4,phantom}} \quad (7)$$

Furthermore, it has also been shown that the spongiosa volume for a healthy person can be estimated from anthropometric measurements such as patient height, or the height and width of the pelvis determined from a CT image [34–36].

Data analysis

The MIRD schema [16, 37] is applied for dosimetry and the total absorbed dose to the bone marrow equals the sum of the contributions from the relevant source regions. The contributions from activity specifically taken up in the bone marrow $\left(\overline{D}_{BM\leftarrow BM}\right)$, the bone $\left(\overline{D}_{BM\leftarrow bone}\right)$ and the remainder of the body $\left(\overline{D}_{BM\leftarrow RoB}\right)$, respectively, should be considered and summed in order to calculate the total absorbed dose to the bone marrow $\left(\overline{D}_{BM}\right)$:

$$\begin{aligned}\overline{D}_{BM} &= \overline{D}_{BM\leftarrow BM} + \overline{D}_{BM\leftarrow bone} + \sum_h \overline{D}_{BM\leftarrow h} + \overline{D}_{BM\leftarrow RoB} = \\ &= \widetilde{A}_{BM} \cdot S_{BM\leftarrow BM} + \widetilde{A}_{bone} \cdot S_{BM\leftarrow bone} + \sum_h \widetilde{A}_h \cdot S_{BM\leftarrow h} \\ &\quad + \widetilde{A}_{RoB} \cdot S_{BM\leftarrow RoB}\end{aligned} \quad (8)$$

The contribution from other major sources organs with a high activity uptake, of which the liver is one example, is included in the term $\sum_h \overline{D}_{BM\leftarrow h}$, and sources of activity distributed elsewhere in the body is gathered in the last term $\overline{D}_{BM\leftarrow RoB}$, for the remainder of the body.

The self-absorbed dose to the bone marrow $\left(\overline{D}_{BM\leftarrow BM}\right)$ is further divided into the contribution from the activity in the bone marrow cells, the blood cells that traverse into the bone marrow space and the extracellular fluid:

$$\begin{aligned}\overline{D}_{BM\leftarrow BM} &= \overline{D}_{BM\leftarrow ECF} + \overline{D}_{BM\leftarrow BLcells} + \overline{D}_{BM\leftarrow BMcells} = \\ &= \left(\widetilde{A}_{ECF} + \widetilde{A}_{BLcells} + \widetilde{A}_{BMcells}\right) \cdot S_{BM\leftarrow BM}\end{aligned} \quad (9)$$

Each of the sections below opens with a more thorough description, and Table 2 gives advice on which source regions to consider for some common radiopharmaceuticals and patient subgroups.

Cumulated activity The cumulated activity $\left(\widetilde{A}_h\right)$, (i.e. the number of decays in the source region) is obtained from the area under the curve describing the activity in the source region as a function of time after administration. The cumulated activity can be calculated by several methods, for example by determination of the integral over time for

an exponential equation fit to the curve (Eqs. 10 and 11), trapezoidal integration and Riemann integration.

$$\widetilde{A}_h = \int_0^\infty A_h(t)dt \tag{10}$$

$$A_h(t) = \sum_j A_{h,j} \cdot e^{-t\left(\lambda_{h,j}+\lambda\right)} \tag{11}$$

where λ is physical decay constant and $\lambda_{h,j}$ the biological disappearance constant for the jth exponential component. The activity corrected to the time of administration of the radiopharmaceutical should be used when the physical decay constant is added separately, as described here. An initial uptake phase of the radiopharmaceutical could be modelled by the application of a negative $A_{h,j}$ in Eq. 11. A good fit to the measured data should be found before the cumulated activity is calculated [38]. The cumulated activity is generally calculated from the time of administration of the radiopharmaceutical to infinity as denoted in Eq. 10.

Extrapolation from the first measurement to time zero (t=0) and extrapolation from the last measurement to infinite time are often needed to determine the total cumulated activity. A useful measure to estimate the uncertainty due to the extrapolations is to calculate the fraction of the cumulated activity that is delivered during the time period of the measurements of the activity, that is the ratio of the cumulated activity for the time interval between the first and the last measurements (t_1 and t_T, respectively) and the total cumulated activity (from zero to infinite time). It is recommended that the fractional contribution (f) from the extrapolations is less than 20%:

$$f = 1 - \left(\frac{\int_{t_1}^{t_T} A(t)dt}{\int_0^\infty A(t)dt} \right) \tag{12}$$

S values Most published S values for bone and bone marrow (ICRP report 30, MIRD pamphlet 11, MIRDOSE2, MIRDOSE3 and OLINDA/EXM [39–42]) use the same source of anatomical data. Spiers et al. determined chord length distributions for the spongiosa (bone marrow cavities and bone trabeculae) for a 44-year-old man and applied the CSDA (continuous slowing down approximation) to calculate absorbed fractions for bone and bone marrow [43–45]. The ICRP 30 S values were based on these calculations. Eckerman and Stabin [46] extended the work of Spiers et al. to more bone regions and applied Berger's energy/range relationship to determine the regional and skeletal averaged S values published in MIRDOSE3 [41] and OLINDA/EXM [42, 47]. Bouchet et al. applied the EGS4/PRESTA radiation transport code to perform Monte Carlo simulations to calculate S values for the Spiers geometry of the bone and bone marrow [48–50]. S values for alpha particles were also determined [51]. Analyses comparing published S values attribute differences to several factors: mass of the target region, and differences in the calculation of the absorbed fractions and weighting schemes for calculation of skeletal averaged S values [50, 52, 53]. Bolch and co-workers have developed skeletal models based on more subjects and have combined macro- and microscopic levels of trabecular bone and marrow cavities (spongiosa) to allow new models to be more patient specific [54].

The S value for the self-absorbed dose is generally scaled according to the mass, whilst the S value for the cross-absorbed dose is considered to be independent of the mass and therefore is not scaled [55]. Previous studies have shown that calculations of absorbed dose to bone marrow that consider the patient-specific bone marrow mass give an improved correlation with toxicity [2, 56] and it is therefore recommended that the S value is scaled to the patient-specific bone marrow mass according to the following equation:

$$S_{(BM\leftarrow BM),patient} = S_{(BM\leftarrow BM),phantom} \cdot \frac{m_{BM,phantom}}{m_{BM,patient}} \tag{13}$$

Self-absorbed dose to the bone marrow $\left(\overline{D}_{BM\leftarrow BM}\right)$

The total self-absorbed dose, on a macroscopic scale, to the bone marrow consists of contributions from activity in the extracellular fluid, blood cells and bone marrow cells (Eq. 9).

Contribution from activity in the extracellular fluid $\left(\overline{D}_{BM\leftarrow ECF}\right)$

The so-called blood method [57] is based on the assumption that the activity concentration in the extracellular space within the bone marrow equals the activity concentration in the plasma. The activity concentration in the bone marrow can therefore be calculated via the activity concentration in plasma combined with the red marrow extracellular fluid fraction, which is assumed to equal 0.19 (RMECFF=0.19) [57]:

$$\overline{D}_{BM\leftarrow ECF} = \left[\widetilde{A}_{plasma}\right] \cdot RMECFF \cdot m_{BM,phantom} \cdot S_{(BM\leftarrow BM),phantom} \tag{14}$$

The cumulated activity is calculated from the curve describing the activity concentration as a function of time

and is denoted $\left[\widetilde{A}_{plasma}\right]$ for plasma, as in Eq. 14 above. It is not necessary to estimate the patient-specific bone marrow mass when the blood method is applied as it cancels out in Eq. 14 when the S value is scaled (due to the use of the activity concentration in blood and plasma). Therefore the S values for the phantom ($S_{(\mathrm{BM}\leftarrow\mathrm{BM}),\mathrm{phantom}}$) must be included rather than a patient-specific S value.

Contribution from activity in blood cells $\left(\overline{D}_{BM\leftarrow BLcells}\right)$

The activity concentration in the blood can also be used to calculate the activity in the bone marrow. The total activity in the blood is the sum of the activity circulating freely in the plasma and the activity uptake in blood cells. The HCT, which expresses the proportion of the blood volume that is occupied by blood cells, can be applied to calculate the activity concentration in the plasma and thereby in the bone marrow if there is no specific activity uptake in blood cells [57]. The activity concentration in the bone marrow can be estimated from the activity concentration in the blood by a factor called the red marrow-to-blood activity concentration ratio (RMBLR):

$$[A]_{plasma} = \frac{[A]_{blood}}{1 - HCT} \tag{15}$$

$$\frac{[A]_{RM}}{[A]_{blood}} = RMBLR = \frac{RMECFF}{1 - HCT} \tag{16}$$

The RMBLR can also be applied if there is a specific activity uptake in blood cells, but the RMBLR will be changed as blood cells are transported into the bone marrow, and Eq. 15 can therefore not be applied. Equation 16 can be applied, although with a modified value for the RMBLR.

The cumulated activity is calculated from the curve describing the activity concentration as a function of time and is denoted $\left[\widetilde{A}_{blood}\right]$ in the following equation:

$$\overline{D}_{BM\leftarrow BLcells} = \left[\widetilde{A}_{blood}\right] \cdot RMBLR \cdot m_{BM,phantom} \cdot S_{BM\leftarrow BM,phantom} \tag{17}$$

As already described, it is not necessary to estimate the patient-specific bone marrow mass when the blood method is applied as it cancels out in Eq. 17 when the S value is scaled (due to the use of the activity concentration), and therefore the S values for the phantom ($S_{\mathrm{BM}\leftarrow\mathrm{BM,phantom}}$) must be included rather than a patient-specific S value.

The RMBLR has been found to be different for different radiopharmaceuticals. Originally the activity concentration in the bone marrow was set to equal the concentration in the blood for radiolabelled monoclonal antibodies, although later this approach was considered as too conservative. Sgouros recommended a RMBLR of 0.36, based on a theoretical investigation of radiolabelled monoclonal antibodies [57], and this value is in line with the recommendations of the AAPM (American Association of Physicists in Medicine) of 0.2–0.4 [58]. A RMBLR of 1 has been found suitable for ^{131}I-NaI [59] as well as for ^{177}Lu-peptide [4]. It has also been shown that the RMBLR might not be constant over time for all radiopharmaceuticals [60].

Contribution from activity in bone marrow cells $\left(\overline{D}_{BM\leftarrow BMcells}\right)$

The activity in the bone marrow cells must be estimated via quantitative imaging of the activity in different regions of the bone marrow. ROIs are drawn over suitable locations on the acquired images and the activity in the ROI is determined. Most commonly the activity in the sacrum [28] or the lumbar vertebrae (L2–L4) [2] is determined, although ROIs over the upper humerus and femur have also been utilized [61]. The total activity in the bone marrow is estimated from the regional uptake by rescaling the fraction of the total bone marrow that is represented by the ROI:

$$\overline{D}_{BM\leftarrow BMcells} = \widetilde{A}_{ROI} \cdot S_{BM\leftarrow BM} / r_{ROI,BM} \tag{18}$$

where $r_{\mathrm{ROI,BM}}$ is the factor rescaling the activity in the bone marrow within the ROI to the whole bone marrow. The fractions of total activity in the bone marrow of various sites are shown in Table 3. However, the amounts in the bone marrow of the different sites vary with age, and Table 3 is only applicable to the healthy adult.

Activity in bone $\left(\overline{D}_{BM\leftarrow bone}\right)$

The activity in bone can be determined from an ROI over the whole body if the activity is only present in bone or from ROIs drawn around single bones, for example left and right femur. The total activity in the skeleton is subsequently determined using the fraction of total bone present within the ROI ($r_{\mathrm{ROI,bone}}$), as shown in Table 4. The value of $r_{\mathrm{ROI,bone}}$ is 1 if an ROI over the whole body is utilized. Alternatively, the regional activity can be used to calculate the absorbed dose to bone marrow for a separate region if regional skeletal S values are applied [46].

The absorbed dose to the red marrow is dependent on the spatial distribution of the radionuclide within the bone:

$$\overline{D}_{BM\leftarrow bone} = \widetilde{A}_{bone} \cdot S_{BM\leftarrow bone} / r_{ROI,bone} \tag{19}$$

There are four factors to consider: (1) amount of activity in trabecular bone, (2) amount of activity in cortical bone, (3) amount of activity uniformly distributed over the bone volume, and (4) amount of activity distributed over the bone surfaces. ICRP Report 30 recommends that the activity is uniformly distributed over the bone volume if the radionuclide in use has a physical half-life longer than

15 days and is uniformly distributed over the bone surfaces if the physical half-life is less (as the activity will decay before it is distributed throughout the bone volume) [40].

Contribution from major organs and the remainder of the body $\left(\overline{D}_{BM\leftarrow h}\right)$

Single major organs can contribute considerably to the total absorbed dose to the bone marrow [4]. The cumulated activity in the source region h can be assessed from quantitative imaging and subsequently multiplied by the relevant S value:

$$\overline{D}_{BM\leftarrow h} = \widetilde{A}_h \cdot S_{BM\leftarrow h} \tag{20}$$

The cumulated activity for the remainder of the body $\left(\widetilde{A}_{RoB}\right)$ is calculated as the difference between the cumulated activity for the whole body and the sum of the cumulated activity in all source regions h except the remainder of the body:

$$\overline{D}_{BM\leftarrow RoB} = \left(\widetilde{A}_{WB} - \sum_h \widetilde{A}_h\right) \cdot S_{BM\leftarrow RoB} \tag{21}$$

The reciprocity theorem (i.e. $S_{k\leftarrow h} = S_{h\leftarrow k}$) is used to calculate the S value for the remainder of the body [55] if the only source regions can assumed to be the bone marrow and the remainder of the body [3, 32, 62] according to the following equation:

$$S_{BM\leftarrow RoB} = \left(S_{BM\leftarrow WB} \cdot \frac{m_{WB,phantom}}{m_{WB,phantom} - m_{BM,phantom}} - S_{BM\leftarrow BM} \cdot \frac{m_{BM,phantom}}{m_{WB,phantom} - m_{BM,phantom}}\right) \cdot \frac{m_{WB,phantom}}{m_{WB,patient}} \tag{22}$$

However, when more than two source regions are involved the generally applicable equation [62] is as follows:

$$S_{BM\leftarrow RoB} = S_{BM\leftarrow WB} \cdot \frac{m_{WB,phantom}}{m_{WB,patient}} \cdot \frac{m_{BM,phantom}}{m_{BM,patient}} - S_{BM\leftarrow BM} \cdot \frac{m_{BM,phantom}}{m_{RoB,patient}} \cdot \frac{m_{BM,phantom}}{m_{BM,patient}} - \tag{23}$$

$$-\sum_h S_{BM\leftarrow h} \cdot \frac{m_{h,phantom}}{m_{Rob,patient}} \cdot \frac{m_{BM,phantom}}{m_{BM,patient}}$$

Note that the mass of the remainder of the body, m_{RoB}, in Eq. 23 equals the mass of the total body minus the sum of the mass of all source regions:

$$m_{RoB} = m_{WB} - m_{BM} - \sum_h m_h \tag{24}$$

Absorbed dose to the whole body $\left(\overline{D}_{WB\leftarrow WB}\right)$

The absorbed dose to the whole body is often used as a surrogate for the absorbed dose to the bone marrow and has been applied in investigations of the relationship between the absorbed dose and the toxic effect on the bone marrow [63–65]. If the activity is assumed to be uniformly distributed, then Eqs. 8 and 13 will be simplified into the calculation of the mean absorbed dose to the whole body:

$$\overline{D}_{BM} \approx \overline{D}_{WB} = \widetilde{A}_{WB} \cdot S_{WB\leftarrow WB} \cdot \frac{m_{WB,phantom}}{m_{WB,patient}} \tag{25}$$

The mean absorbed dose to the whole body should be calculated from measurements of the activity in the whole body. The self-absorbed S value for the phantom should be scaled by the whole body weight to improve the accuracy in the calculated absorbed dose [66].

General remarks

The dosimetry methods discussed here can be considered as a robust baseline, although more sophisticated dosimetry methods could be applied, for example activity quantification on a voxel level, activity quantification from PET, PET/CT and SPECT/CT images and patient-specific 3-D voxel-based calculations of the absorbed dose, by either convolution with a dose-point kernel or Monte Carlo simulations.

The methods may be used to calculate the mean absorbed dose over the whole bone marrow compartment. A nonuniform absorbed dose might be caused by a nonuniform activity distribution within the bone marrow itself or by the cross-absorbed dose from major tissues other than the bone marrow. It is, however, recommended

Table 3 The percentage of total red marrow present at different skeletal sites in a healthy adult [11, 13]

Skeletal site	Percentage of red marrow
Cranium	7.6
Mandible	0.8
Scapulae	2.8
Clavicles	0.8
Sternum	3.1
Ribs	16.1
Cervical vertebrae	3.9
Thoracic vertebrae	16.1
Lumbar vertebrae	12.3
Sacrum	9.9
Os coxae	17.5
Femora, upper half	6.7
Femora, lower half	0
Tibiae, fibulae, patellae	0
Ankle and foot bones	0
Humeri, upper half	2.3
Humeri, lower half	0
Ulnae, radii	0
Wrist and hand bones	0

that the average over multiple regional sites, together with the minimum and maximum, should be calculated if the bone marrow uptake is noticeably inhomogeneous.

A nonuniform absorbed dose can also be a result of differences in scattering properties close to the interfaces between bone and soft tissue [67, 68]. The cellularity of different macroscopic bone marrow regions varies in the healthy adult, and treatment with external beam radiotherapy might increase the variation. Inclusion of bone marrow cellularity in the calculations could be considered [32, 47, 51], but it has been shown that cellularity is only of importance for low-energy electrons so the relatively small impact of using the patient-specific cellularity may not justify the extra cost. Furthermore, the distribution of bone marrow stem cells is not uniform within the bone marrow cavities in the trabecular bone. Watchman et al. [69] found a linear relationship between the concentration of haematopoietic stem cells and distance from the trabecular bone surface.

The absorbed dose, i.e. the deposited energy per unit mass, is inversely proportional to the mass of the target region. However, the macroscopic mass of the bone marrow is difficult to determine because of its anatomical spread throughout the body. Newer image-based methods for estimating bone marrow mass include MRI [70] and PET, via either ^{52}Fe [71] or ^{18}F-FLT [72].

A bone marrow biopsy could be performed to help determine the activity uptake in the bone marrow, although this is associated with uncertainties [57] and only gives the activity concentration in bone marrow at one location. A bone marrow biopsy could also be performed to determine the expression of a target antigen via flow cytometry.

Determination of the relationship between absorbed dose and biological effect is dependent not only on the accuracy in the assessment of absorbed dose, but also on the accuracy in the assessment of the biological effect (toxicity). The haematological toxicity assessed from blood cell counts in the peripheral blood is used as a surrogate measure of the true radiation damage to the haematopoietic stem cells. However, the true bone marrow toxicity should be assessed in terms of the damage to the stem cells which produce all blood cells, as the decrease in the number of peripheral blood cells could be affected by both direct cell death caused by irradiation of the cells in the blood and the delayed effect of the decrease in production of the blood cells. The haematological toxicity is often assessed via fixed grades according to toxicity schemes such as the RTOG or the WHO grading schemes, and the choice of toxicity scheme may influence the relationship between absorbed dose and effect. Therefore, these relationships should be established from values based on the percentage decrease from a baseline value of the number of blood cells.

The level of the cytokine FLT3-L has been used as a factor in predicting the state of recovery of the bone marrow stem cells following toxic treatments, and thereby their sensitivity to radiation [73–75]. Furthermore, the microscopic structure of the bone marrow has been shown to be perturbed after irradiation, raising the question of whether the bone marrow damage is only due to the death of stem cells [15].

Table 4 Weight of individual bones expressed as percent of the total weight of the skeleton [12]

Bone	Male	Female
Skull	11.8±1.6	11.9±0.8
Mandible	1.2±0.2	1.2±0.2
Vertebrae and sacrum	19.0±1.6	20.4±1.5
Ribs	7.0±0.4	5.6±0.4
Sternum	1.2±0.2	1.2±0.2
Femora	15.3±1.5	15.9±0.7
Tibiae and fibulae	11.3±1.4	11.9±0.7
Pelvic bones	10.6±0.8	10.5±1.0
Feet	6.3±0.7	6.8±0.5
Humeri	5.3±0.5	4.7±0.4
Radii and ulnae	3.6±0.6	3.2±0.3
Scapulae	3.6±0.2	2.9±0.2
Hands	2.3±0.3	2.4±0.5
Clavicles	0.8±0.1	0.7±0.1
Patellae	0.7±0.1	0.6±0.1

Acknowledgments This work was developed under the close supervision of the Dosimetry Committee of the EANM (M. Bardiès, C. Chiesa, G. Flux, M. Konijnenberg, M. Lassmann, M. Monsieurs, S.-E. Strand). In addition, the authors wish to acknowledge the contribution from S. Savolainen, past member of the EANM Dosimetry Committee.

References

1. Wahl RL, Zasadny K, MacFarlane D, et al. Iodine-131 anti-B1 antibody for B-cell lymphoma: an update on the Michigan Phase I experience. J Nucl Med 1998;39(8 Suppl):21S–7S.
2. Shen S, Meredith RF, Duan J, et al. Improved prediction of myelotoxicity using a patient-specific imaging dose estimate for non-marrow-targeting ^{90}Y-antibody therapy. J Nucl Med 2002;43 (9):1245–53.
3. Wessels BW, Bolch WE, Bouchet LG, et al. Bone marrow dosimetry using blood-based models for radiolabeled antibody therapy: a multiinstitutional comparison. J Nucl Med 2004;45 (10):1725–33.
4. Forrer F, Krenning EP, Kooij PP, et al. Bone marrow dosimetry in peptide receptor radionuclide therapy with [^{177}Lu-DOTA(0),Tyr (3)]octreotate. Eur J Nucl Med Mol Imaging 2009;36(7):1138–46.
5. Breitz HB, Fisher DR, Wessels BW. Marrow toxicity and radiation absorbed dose estimates from rhenium-186-labeled monoclonal antibody. J Nucl Med 1998;39(10):1746–51.
6. Shen S, Meredith RF, Duan J, et al. Comparison of methods for predicting myelotoxicity for non-marrow targeting I-131-antibody therapy. Cancer Biother Radiopharm 2003;18(2):209–15.
7. O'Donoghue JA, Baidoo N, Deland D, et al. Hematologic toxicity in radioimmunotherapy: Dose-response relationships for 131-I labeled antibody therapy. Cancer Biother Radiopharm 2002;17 (4):435–43.
8. Behr T, Béhé M, Sgouros G. Correlation of red marrow radiation dosimetry with myelotoxicity: Empirical factors influencing the radiation-induced myelotoxicity of radiolabeled antibodies, fragments and peptides in pre-clinical and clinical settings. Cancer Biother Radiopharm 2002;17(4):445–64.
9. Hindorf C, Lindén O, Tennvall J, et al. Evaluation of methods for red marrow dosimetry based on patients undergoing radioimmunotherapy. Acta Oncol 2005;44:579–88.
10. Lindén O, Tennvall J, Hindorf C, et al. ^{131}I-labelled anti-CD22 MAb (LL2) in patients with B-cell lymphomas failing chemotherapy. Treatment outcome, haematologic toxicity and absorbed dose to bone marrow. Acta Oncol 2002;41(3):297–303.
11. International Commission on Radiological Protection, Basic anatomical and physiological data for use in radiological protection: the skeleton. 1995, Pergamon: Oxford, UK
12. International Commission on Radiological Protection, Basic anatomical and physiological data for use in radiological protection: reference values. 2002, Pergamon: Oxford, UK
13. Cristy M. Active bone marrow distribution as a function of age in humans. Phys Med Biol 1981;26(3):389–400.
14. Bradley EW. Bone marrow physiology and radiobiology. Antibody Immunoconjug Radiopharm 1990;3(4):289–91.
15. Fliedner TM, Graessle D, Paulsen C, et al. Structure and function of bone marrow hemopoiesis: mechanisms of response to ionizing radiation exposure. Cancer Biother Radiopharm 2002;17(4):405–26.
16. Loevinger R, Budinger TF, Watson EE. MIRD primer for absorbed dose calculations. New York: The Society of Nuclear Medicine; 1991.
17. Siegel JA, Thomas SR, Stubbs JB, et al. MIRD Pamphlet No 16: Techniques for quantitative radiopharmaceutical biodistribution data acquisition and analysis for use in human radiation dose estimates. J Nucl Med 1999;40(2):37s–61s.
18. Chittenden S, Pratt BE, Pomeroy K, et al. Optimization of equipment and methodology for whole body activity retention measurements in children undergoing targeted radionuclide therapy. Cancer Biother Radiopharm 2007;22 (2):243–9.
19. He B, Wahl RL, Du Y, et al. Comparison of residence time estimation methods for radioimmunotherapy dosimetry and treatment planning – Monte Carlo simulation studies. IEEE Trans Med Imaging 2008;27(4):521–30.
20. Koral K, Dewaraja Y, Li J, et al. Initial results for hybrid SPECT – conjugate-view tumor dosimetry in ^{131}I-anti-B1 antibody therapy of previously untreated patients with lymphoma. J Nucl Med 2000;41(9):1579–86.
21. Sgouros G, Kolbert K, Sheikh A, et al. Patient-specific dosimetry for ^{131}I thyroid cancer therapy using ^{124}I PET and 3-dimensional-internal dosimetry (3D-ID) software. J Nucl Med 2004;45 (8):1366–72.
22. Hobbs RF, Wahl RL, Lodge MA, et al. ^{124}I PET-based 3D-RD dosimetry for a pediatric thyroid cancer patient: real-time treatment planning and methodologic comparison. J Nucl Med 2009;50(11):1844–7.
23. Perk LR, Visser OJ, Stigter-van Walsum M, et al. Preparation and evaluation of ^{89}Zr-Zevalin for monitoring of ^{90}Y-Zevalin biodistribution with positron emission tomography. Eur J Nucl Med Mol Imaging 2006;33:1337–45.
24. Ogawa K, Harata Y, Ichihara T, et al. A practical method for position-dependent Compton-scatter correction in single photon emission CT. IEEE Trans Med Imaging 1991;10(3):408–12.
25. Macey DJ, Grant EJ, Bayouth JE, et al. Improved conjugate view quantitation of I-131 by subtraction of scatter and septal penetration events with a triple energy window method. Med Phys 1995;22(10):1637–43.
26. Fleming JS. A technique for the measurement of activity using a gamma camera and computer. Phys Med Biol 1979;24(1):176–80.
27. Thomas SR, Maxon HR, Kereiakes JG. In vivo quantitation of lesion radioactivity using external counting methods. Med Phys 1976;3(4):253–5.
28. Siegel JA, Lee RE, Pawlyk DA, et al. Sacral scintigraphy for bone marrow dosimetry in radioimmunotherapy. Nucl Med Biol 1989; 16(6):553–9.
29. Chang LT. A method for attenuation correction in radionuclide computed tomography. IEEE Trans Nucl Sci 1978;25:638–43.
30. Shepp LA, Vardi Y. Maximum likelihood reconstruction for emission tomography. IEEE Trans Med Imaging 1982;1:113–22.
31. Lange K, Carson R. EM reconstruction algorithms for emission and transmission tomography. J Comp Assist Tomogr 1984;8: 306–16.
32. Stabin MG, Siegel JA, Sparks RB. Sensitivity of model-based calculations of red marrow dosimetry to changes in patient-specific parameters. Cancer Biother Radiopharm 2002;17(5):535–43.
33. Bolch WE, Patton PW, Shah AP, et al. Considerations of anthropomorphic, tissue volume, and tissue mass scaling for improved patient specificity of skeletal S values. Med Phys 2002;29:1054–70.
34. Brindle JM, Myers SL, Bolch WE. Correlations of total pelvic spongiosa volume with both anthropometric parameters and computed tomography-based skeletal size measurements. Cancer Biother Radiopharm 2006;21(4):352–63.
35. Brindle JM, Trindade AA, Shah AP, et al. Linear regression model for predicting patient-specific total skeletal spongiosa volume for use in molecular radiotherapy dosimetry. J Nucl Med 2006;47 (11):1875–83.
36. Pichardo JC, Trindade AA, Brindle JM, et al. Method for estimating skeletal spongiosa volume and active marrow mass in the adult male and adult female. J Nucl Med 2007;48 (11):1880–8.

37. Bolch WE, Eckerman KF, Sgouros G, et al. MIRD Pamphlet No. 21: a generalized schema for radiopharmaceutical dosimetry – standardization of nomenclature. J Nucl Med 2009;50(3):477–84.
38. Glatting G, Kletting P, Reske SN, et al. Choosing the optimal fit function: Comparison of the Akaike information criterion and the F-test. Med Phys 2007;34(11):4285–92.
39. Snyder WS, Ford MR, Warner GG, et al. "S", absorbed dose per unit cumulated activity for selected radionuclides and organs. New York: The Society of Nuclear Medicine; 1975.
40. ICRP Publication 30, Part 1, Limits for intakes of radionuclides by workers. Ottawa: International Commission on Radiological Protection. 1980
41. Stabin MG. MIRDOSE: personal computer software for internal dose assessment in nuclear medicine. J Nucl Med 1996;37 (3):538–46.
42. Stabin MG, Sparks RB, Crowe E. OLINDA/EXM: The second-generation personal computer software for internal dose assessment in nuclear medicine. J Nucl Med 2005;46(6):1023–7.
43. Beddoe AH, Darley PJ, Spiers FW. Measurements of trabecular bone structure in man. Phys Med Biol 1976;21(4):589–607.
44. Beddoe AH. Measurements of the microscopic structure of cortical bone. Phys Med Biol 1977;22(2):298–308.
45. Whitwell JR, Spiers FW. Calculated beta-ray dose factors for trabecular bone. Phys Med Biol 1976;21(1):16–38.
46. Eckerman KF, Stabin MG. Electron absorbed fractions and dose conversion factors for red marrow and bone by skeletal regions. Health Phys 2000;78(2):199–214.
47. Stabin MG, Siegel JA. Physical models and dose factors for use in internal dose assessment. Health Phys 2003;85(3):294–310.
48. Bouchet LG, Bolch WE. A three-dimensional transport model for determining absorbed fractions of energy for electrons within cortical bone. J Nucl Med 1999;40(12):2115–24.
49. Bouchet LG, Jokisch DW, Bolch WE. A three-dimensional transport model for determining absorberd fractions of energy for electrons within trabecular bone. J Nucl Med 1999;40 (11):1947–66.
50. Bouchet LG, Bolch WE, Howell RW, et al. S values for radionuclides localized within the skeleton. J Nucl Med 2000;41 (1):189–212.
51. Watchman CJ, Jokisch DW, Patton PW, et al. Absorbed fractions for alpha-particles in tissues of trabecular bone: considerations of marrow cellularity within the ICRP reference male. J Nucl Med 2005;46(7):1171–85.
52. Stabin MG, Eckerman KF, Bolch WE, et al. Evolution and status of bone and marrow dose models. Cancer Biother Radiopharm 2002;17(4):427–33.
53. Sgouros G, Stabin M, Erdi Y, et al. Red marrow dosimetry for radiolabeled antibodies that bind to marrow, bone, or blood components. Med Phys 2000;27(9):2150–64.
54. Shah AP, Bolch WE, Rajon DA, et al. A paired-image radiation transport model for skeletal dosimetry. J Nucl Med 2005;46 (2):344–53.
55. Petoussi-Henss N, Bolch WE, Zankl M, et al. Patient-specific scaling of reference S-values for cross-organ radionuclide S-values: What is appropriate? Radiat Prot Dosim 2007;127:192–6.
56. Shen S, DeNardo GL, Sgouros G, et al. Practical determination of patient-specific marrow dose using radioactivity concentration in blood and body. J Nucl Med 1999;40(12):2102–6.
57. Sgouros G. Bone marrow dosimetry for radioimmunotherapy: theoretical considerations. J Nucl Med 1993;34(4):689–94.
58. Siegel JA, Wessels BW, Watson EE, et al. Bone marrow dosimetry and toxicity for radioimmunotherapy. Antibody Immunoconjug Radiopharm 1990;3(4):213–33.
59. Sgouros G. Blood and bone marrow dosimetry in radioiodine therapy of thyroid cancer. J Nucl Med 2005;46(5):899–900.
60. Hindorf C, Lindén O, Tennvall J, et al. Time dependence of activity concentration ratio of red marrow to blood and implications for red marrow dosimetry. Cancer 2002;94(4 suppl):1235–9.
61. Sgouros G, Jureidini IM, Scott AM, et al. Bone marrow dosimetry: regional variability of marrow-localizing antibody. J Nucl Med 1996;37:695–8.
62. Traino AC, Ferrari M, Cremonesi M, et al. Influence of total-body mass on the scaling of S-factors for patient-specific, blood-based red-marrow dosimetry. Phys Med Biol 2007;52:5231–48.
63. Matthay KK, Panina C, Huberty J, et al. Correlation of tumor and whole-body dosimetry with tumor response and toxicity in refractory neuroblastoma treated with ^{131}I-MIBG. J Nucl Med 2001;42(11):1713–21.
64. Buckley SE, Chittenden S, Saran FH, et al. Whole-body dosimetry for individualized treatment planning of ^{131}I-MIBG radionuclide therapy for neuroblastoma. J Nucl Med 2009;50 (9):1518–24.
65. Seldin DW. Techniques for using bexxar for the treatment of non-Hodgkin's lymphoma. J Nucl Med Technol 2002;30(3): 109–14.
66. Divoli A, Chiavassa S, Ferrer L, et al. Effect of patient morphology on dosimetric calculations for internal irradiation as assessed by comparisons of Monte Carlo versus conventional methods. J Nucl Med 2009;50(2):316–23.
67. Kwok CS. Backscattering of low energy electrons at bone/bone marrow interfaces. Antibody Immunoconjug Radiopharm 1990;3 (4):251–7.
68. Kwok CS, Bialobzyski PJ, Yu SK. Effect of tissue inhomogneity on dose distribution of continuous activity of low-energy electrons in bone marrow cavities with different topologies. Med Phys 1991;18(3):533–41.
69. Watchman CJ, Bourke VA, Lyon JR, et al. Spatial distribution of blood vessels and CD34+ hematopoietic stem and progenitor cells within the marrow cavities of human cancellous bone. J Nucl Med 2007;48(4):645–54.
70. Daldrup-Link HE, Henning T, Link TM. MR imaging of therapy-induced changes of bone marrow. Eur Radiol 2007;17:743–61.
71. Beshara S, Sörensen J, Lubberink M, et al. Pharmacokinetics and red cell utilization of ^{52}Fe/^{59}Fe-labelled iron polymaltose in anaemic patients using positron emission tomography. Br J Haematol 2003;120:853–9.
72. Agool A, Schot BW, Jager PL, et al. ^{18}F-FLT PET in hematologic disorders: a novel technique to analyze the bone marrow compartment. J Nucl Med 2006;47(10):1592–8.
73. Blumenthal RD, Lew W, Juweid M, et al. Plasma FLT3-L levels predict bone marrow recovery from myelosuppressive therapy. Cancer 2000;88(2):333–43.
74. Siegel JA, Yeldell D, Goldenberg DM, et al. Red marrow radiation dose adjustment using plasma FLT3-L cytokine levels: improved correlations between hematologic toxicity and bone marrow dose for radioimmunotherapy patients. J Nucl Med 2003;44(1):67–76.
75. Bertho JM, Demarquay C, Frick J, et al. Level of flt3-level in plasma: a possible new bio-indicator for radiation-induced aplasia. Int J Radiat Biol 2001;77(6):703–12.